6044 *Organometallics* **2009,** *28,* 6044–6053
DOI: 10.1021/om900435y

ORGANOMETALLICS
Article

Application of Tautomerism of Ferrocenyl Secondary Phosphine Oxides in Suzuki−Miyaura Cross-Coupling Reactions

Lin-Ying Jung, Shih-Hung Tsai, and Fung-E Hong*

Department of Chemistry, National Chung Hsing University, 250 Kuo-Kuang Road, Taichung 40227, Taiwan, Republic of China

Received May 24, 2009

Several new ferrocenyl secondary phosphine oxides, (η^5-C_5H_4-P(=O)(Ph)(H))$_2$Fe (**7aB**) and (η^5-C_5H_4-P(=O)(R)(H))(η^5-C_5H_5)Fe (**7M**, **a**: R = Ph; **c**: R = Cy), were prepared and characterized by spectroscopic means. Further reaction of Pd(COD)Cl_2 with 2 molar equiv of (η^5-C_5H_4-P(=O)-(R)(H))$_2$Fe (**7bM**, **b**: R = ^{t}Bu) led to the formation of the palladium dimer [(**7b′M**)(**7b′M-H**$^+$)Pd(μ-Cl)]$_2$, **8**. In addition, the reaction of Pd(OAc)$_2$ with 1 molar equiv of **7bM** yielded a bis-**7bM**-coordinated palladium acetate, [(**7b′M**)(**7b′M-H**$^+$)Pd(OAc)], **9**. The molecular structures of **7aB**, **7aM**, **7bM**, **8**, and **9** were determined by single-crystal X-ray diffraction methods. A tautomeric equilibrium between **7aB** and its isomeric form (η^5-C_5H_4-P(OH)(Ph))$_2$Fe (**7a′B**) indeed took place. This was also true for the case of **7aM** and its isomeric form (η^5-C_5H_4-P(OH)(Ph))(η^5-C_5H_5)Fe (**7a′M**). Palladium-catalyzed Suzuki−Miyaura reactions employing **7aB** and **7bM** as ligands gave satisfactory results.

1. Introduction

Over the last few decades, the realm of organic synthesis has experienced prolific and beneficial development of transition metal-catalyzed cross-coupling reactions.[1] Among these fascinating synthetic methods, the Suzuki−Miyaura reaction is probably the most commonly employed technique in the formation of carbon−carbon bonds. This reaction is characterized by a coupling process between an aryl halide (or triflate) and organoborate, catalyzed by a ligand-assisted palladium complex in basic medium.[2] The success of the Suzuki−Miyaura coupling can be ascribed to several beneficial factors: (1) low toxicity of organoborates and their byproduct; (2) commercial availability of diverse forms of boronic acids and esters; (3) tolerable stability toward air and water.[3]

A tautomeric equilibrium between a secondary phosphine oxide (RR′HP(=O), **1a**) and its less stable phosphinous acid form (RR′POH, **1b**) is well known (Scheme 1).[4] It is the phosphinous acid form **1b** that exhibits good coordinating capability toward low-valent transition metals. In the presence of base or transition metals, the balance might shift from **1a** to **1b**, then to **1cM**. Satisfactory catalytic performances for palladium-catalyzed cross-coupling reactions employing **1b**-like phosphine ligands have been reported.[5]

There are few published studies of the tautomerism of a metal-containing phosphine oxide and the corresponding phosphinous acid.[6] Since the reactivity of the cyclopentadinyl ring of the ferrocene has been well studied, modification on the rings should be readily achievable. In this work, we report the preparation of several iron-containing secondary

*To whom correspondence should be addressed. Fax: 886-4-22862547. E-mail: fehong@dragon.nchu.edu.tw.

(1) (a) Alberico, D.; Scott, M. E.; Lautens, M. *Chem. Rev.* **2007**, *107*, 174–238. (b) Corbet, J.-P.; Mignani, G. *Chem. Rev.* **2006**, *106*, 2651–2710. (c) Hassan, J.; Sévingnon, M.; Gozzi, C.; Schulz, E.; Lemaire, M. *Chem. Rev.* **2002**, *102*, 1359–1469. (d) Houk, K. N.; Sessler, H.; Lehn, J.-M.; Ley, S. V.; de Meijere, A.; Schreiber, S. L.; Thiem, J.; Trost, B. M.; Vögtle, F.; Yamamoto, H., Eds. *Cross-Coupling Reactions−A Practical Guide in Topics in Current Chemistry*; Springer-Verlag: Heidelberg, 2002; Vol. *219*.

(2) (a) Espinet, P.; Echavarren, A. M. *Angew. Chem., Int. Ed.* **2004**, *43*, 4704–4734. (b) Littke, A. F.; Fu, G. C. *Angew. Chem., Int. Ed.* **2002**, *41*, 4176–4211. (c) Miyaura, N.; Suzuki, A. *Chem. Rev.* **1995**, *95*, 2457–2483.

(3) (a) Over 470 boronic acids and their derivatives are listed in the Alfa Aesar brochure *Boronic Acids-Properties and Applications*; Alfa Aesar: Germany, 2008. (b) Hall, D. G., Ed. *Boronic Acids*; Wiley-VCH: Weinheim, 2005. (c) Chemler, S. R.; Trauner, D.; Danishefsky, S. J. *Angew. Chem., Int. Ed.* **2001**, *40*, 4544–4568. (d) Tsuji, J. *Palladium Reagents and Catalysts: New Perspectives for the 21st Century*; John Wiley & Sons Ltd: England, 2004.

(4) (a) Dixon, K. R.; Rattray, A. D. *Can. J. Chem.* **1971**, *49*, 3997–4004. (b) Silver, B.; Luz, Z. *J. Am. Chem. Soc.* **1962**, *84*, 1091–1905. (c) Luz, Z.; Silver, B. *J. Am. Chem. Soc.* **1962**, *84*, 1095–1098. (d) Doak, G. O.; Freedman, L. D. *Chem. Rev.* **1961**, *61*, 31–44. (e) Luz, Z.; Silver, B. *J. Am. Chem. Soc.* **1961**, *83*, 4518–4521.

(5) (a) Yang, D. X.; Colletti, S. L.; Wu, K.; Song, M.; Li, G. Y.; Shen, H. C. *Org. Lett.* **2009**, *11*, 381–384. (b) Pryjomska, I.; Bechowski, H. B.; Ciunik, Z.; Trzeciak, A. M.; Ziółkowski, J. J. *Dalton Trans.* **2006**, 213–220. (c) Ackermann, L.; Born, R.; Spatz, J. H.; Meyer, D. *Angew. Chem.* **2005**, *117*, 7382–7386. *Angew. Chem., Int. Ed.* **2005**, *44*, 7216−7219. (d) Ackermann, L.; Born, R. *Angew. Chem.* **2005**, *117*, 2497–2500. *Angew. Chem., Int. Ed.* **2005**, *44*, 2444-2447. (e) Wolf, C.; Lerebours, R. *Org. Lett.* **2004**, *6*, 1147–1150. (f) Li, G. Y. *J. Org. Chem.* **2002**, *67*, 3643–3650. (g) Li, G. Y. *Angew. Chem.* **2001**, *113*, 1561–1564. *Angew. Chem., Int. Ed.* **2001**, *40*, 1513−1516. (h) Li, G. Y.; Zheng, G.; Noonan, A. F. *J. Org. Chem.* **2001**, *66*, 8677–8681.

(6) (a) Xu, H.; Ekoue-Kovi, K.; Wolf, C. *J. Org. Chem.* **2008**, *73*, 7638–7650. (b) Ekoue-Kovi, K.; Xu, H.; Wolf, C. *Tetrahedron Lett.* **2008**, *49*, 5773–5776. (c) Wei, C.-H.; Wu, C.-E.; Huang, Y.-L.; Kultyshev, R. G.; Hong, F.-E. *Chem.—Eur. J.* **2007**, *13*, 1583–1593. (d) Ackermann, L. *Synlett* **2007**, 507–526. (e) Ackermann, L. *Synthesis* **2006**, 1557–1574. (f) Ackermann, L.; Gschrei, C. J.; Althammer, A.; Riederer, M. *Chem. Commun.* **2006**, 1419–1421. (g) Wolf, C.; Ekoue-Kovi, K. *Eur. J. Org. Chem.* **2006**, 1917–1925.

 Published on Web 09/23/2009

Scheme 1. Tautomeric Equilibrium between a Secondary Phosphine Oxide 1a and Phosphinous Acid 1b as Well As in the Presence of Base and Transition Metal

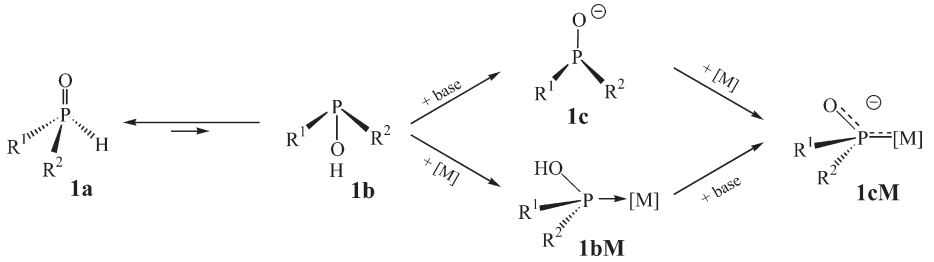

Scheme 2. Preparations of Ferrocenyl Phosphine Oxides and Their Tautomeric Phosphinous Acids[a]

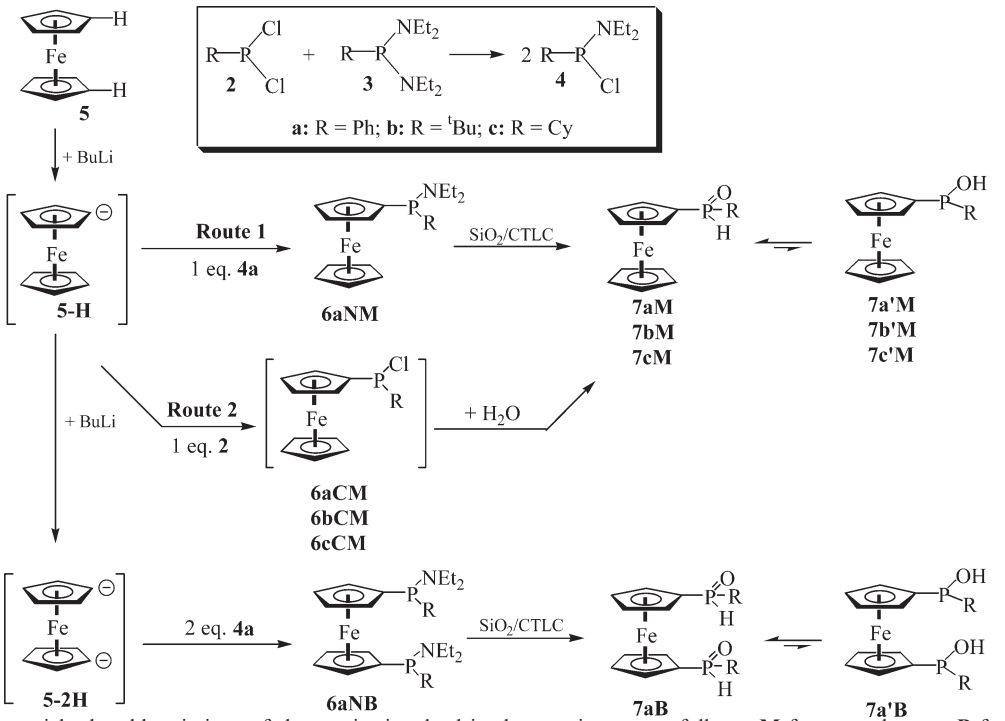

[a] Throughout the article the abbreviations of the species involved in the reaction are as follows: **M** for **m**onodentate; **B** for **b**identate; **N** for diethylamino; **C** for **c**hloride; **a** for R = Ph; **b** for R = ^{t}Bu; **c** for R = Cy; $'$ for phosphinous acid form.

Scheme 3

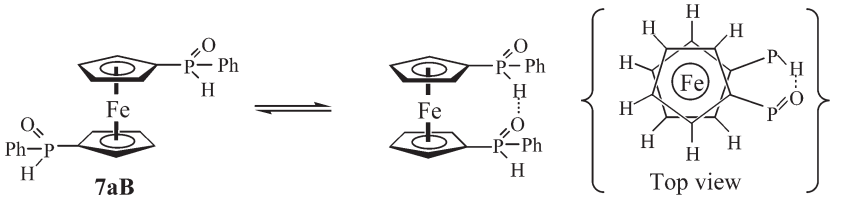

phosphine oxides and the exploration of their catalytic performance in the Suzuki−Miyaura reaction.

2. Results and Discussion

2.1. Preparations of (η^5-C_5H_5)(η^5-C_5H_4-P(NEt_2)(Ph))Fe, 6aNM, and (η^5-C_5H_4-P(NEt_2)(Ph))$_2$Fe, 6aNB. A mono-phosphino-subtituted ferrocene, (η^5-C_5H_5)(η^5-C_5H_4−P(NEt_2)(Ph))Fe, **6aNM**, and diphosphino-subtituted ferrocene, (η^5-C_5H_4-P(NEt_2)(Ph))$_2$Fe, **6aNB**, were prepared by procedures modified from the literature (Scheme 2).[7] First, ferrocene was deprotonated by equimolar amounts of ^{n}BuLi; this was followed by adding equal moles of PPhCl(NEt_2), **4a**. Compounds **6aNM** and **6aNB** were yielded in good quantity. The ^{31}P NMR spectra of **6aNM** and **6aNB** display signals at 55.0 and 54.2 ppm, respectively. The conversion of **6aNB** (or **6aNM**) to its corresponding secondary phosphine oxide (η^5-C_5H_4-P(=O)(Ph)(H))$_2$Fe (**7aB**) (or (η^5-C_5H_5)(η^5-C_5H_4-P(=O)(Ph)(H))Fe, **7aM**) was achieved in acidic media according to the ingenious preparative procedure described by Denis.[7] The corresponding **6bNB** (or **7bB**) could not be made by the same procedure probably due to severe steric hindrance between the two bulky substituents.

(7) (a) Baba, G.; Pilard, J.-F.; Tantaoul, K.; Gaumont, A.-C.; Denis, J.-M. *Tetrahedron Lett.* **1995**, *36*, 4421–4424. (b) Pilard, J.-F.; Baba, G.; Gaumont, A.-C.; Denis, J.-M. *Synlett* **1995**, 1168–1170.

Compound **7aB** was characterized by spectroscopic methods. There are eight discrete signals being observed for the cyclopentadienyl protons in the ^{1}H NMR. This implies that these two cyclopentadienyl rings are not in an equivalent environment. Presumably, an intramolecular hydrogen bonding takes place between the two phosphino substituents that causes discrete chemical shifts for the hydrogen atoms (Scheme 3). The existence of P−H bonds in **7aB** is also evidenced by two sets of large coupling constants (J_{P-H} = 487.3 and 489.3 Hz) between them.

Fortunately, crystals of **7aB** were grown from the CH_2Cl_2 solution, and the structure was determined by single-crystal X-ray diffraction methods. The ORTEP diagram of **7aB** depicted in Figure 1 shows the presence of a ferrocenyl secondary phosphine oxide. The presence of a P═O bond is also evidenced by its short bond length, 1.504(5) Å. The two phosphino groups are situated on the opposite ends of the molecule (Figure 1). Interestingly, the crystal structure does not confirm the required geometry to support the existence of intramolecular hydrogen bonding. The ^{31}P NMR spectrum of **7aB** displays only one signal at 19.2 ppm, which reflects the fact that ^{31}P NMR is not as sensitive as ^{1}H NMR to a small environmental variation.

In principle, a tautomeric equilibrium between **7aB** and the less stable secondary phosphinous acid **7a′B** could take place in solution. Nevertheless, the **7aB** form must be strongly favored in the tautomeric equilibrium without the presence of base or metal, judging from the pattern of the ^{31}P NMR spectrum with a large J_{P-H} coupling constant. Theoretically, **7a′B** could act as a bidentate ligand toward a palladium complex. Therefore, the coordination of **7a′B** to palladium in basic media could yield a catalyst precursor that is ready for the forthcoming coupling reactions (Scheme 2).

The ^{31}P NMR spectra of **6aNM** and **7aM** display signals at 55.0 and 19.8 ppm, respectively. As expected, the chemical shift of **7aM** is close to that of **7aB**. The crystal structure of **7aM** was determined by X-ray diffraction methods. The ORTEP drawing of **7aM** shows the presence of a ferrocenyl secondary phosphine oxide (Figure 2). A tautomeric equilibrium between **7aM** and its less stable secondary phosphinous acid **7a′M** in solution is evidenced by the formation of palladium complexes by using **7a′M** as the coordinating ligand. This will be demonstrated later. Therefore, **7a′M** is able to act as a monodentate ligand in palladium-catalyzed cross-coupling reactions.

2.2. Preparations of (η^5-C_5H_4-P(Cl)(^{t}Bu))(η^5-C_5H_5)Fe, 6bCM, and (η^5-C_5H_4-P(Cl)(Cy))(η^5-C_5H_5)Fe, 6cCM. An alternative preparation of monophosphino-subtituted ferrocenes (η^5-C_5H_4-P(═O)(R)(H))(η^5-C_5H_5)Fe (**7M**, **a**: R = Ph; **b**: R = ^{t}Bu; **c**: R = Cy) can be achieved by taking route 2 (Scheme 2). First, ferrocene was deprotonated by equimolar amounts of BuLi, followed by adding equal moles of $PRCl_2$ **2**. The formation of **6aCM** (or **6bCM** and **6cCM**) was completed within 24 h. The conversion of **6aCM** (or **6bCM** and **6cCM**) to its corresponding **7aM** (or **7bM** and **7cM**) is readily done by adding water. Compounds **7aM**, **7bM**, and **7cM** were yielded in good quantity. The ^{31}P NMR spectra of **7aM**, **7bM**, and **7cM** display signals at 19.8, 47.5, and 37.3 ppm, respectively. The ^{1}H NMR spectra of **7aM**, **7bM**, and 7cM show matching signals for cyclopentadienyl rings at 4.33, 4.36, and 4.36 ppm. The chemical shifts of the phosphorus attached protons (P−H) vary with the surrounding environments and have large coupling constants. They are 8.03 (J_{P-H} = 483.3 Hz), 6.88 (J_{P-H} = 454.5 Hz), and 7.06 (J_{P-H} = 458.5 Hz) for **7aM**, **7bM**, and **7cM**, respectively.

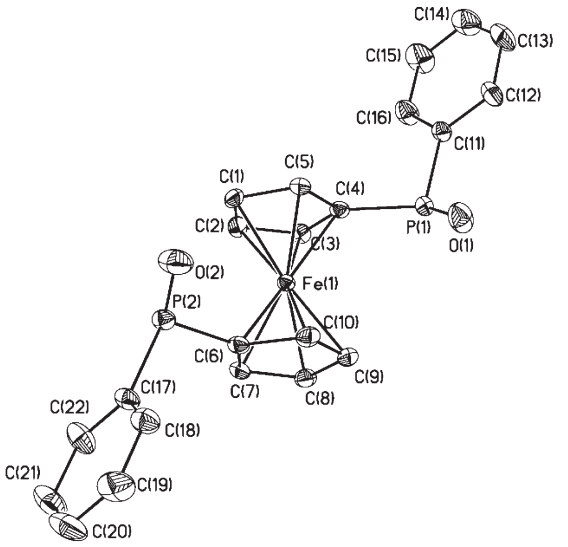

Figure 1. ORTEP drawing of **7aB**. Hydrogen atoms are omitted for clarity.

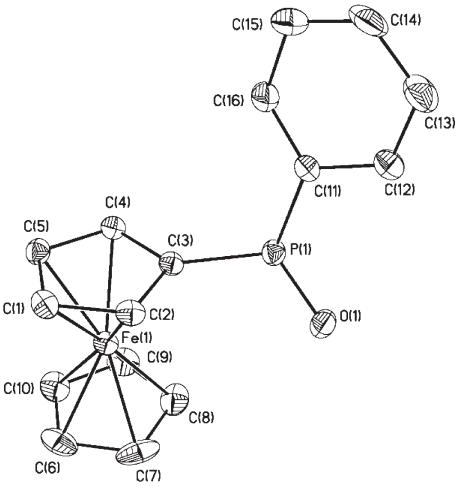

Figure 2. ORTEP drawing of **7aM**. Hydrogen atoms are omitted for clarity.

A tautomeric equilibrium between **7bM** and its less stable secondary phosphinous acid **7b′M** in solution is evidenced by the formation of palladium complexes via **7b′M** as the coordinating ligand. Compound **7bM** has been reported; however, no crystal structure was available.[8,6a] Fortunately, we were able to obtain crystals of **7bM**, and its structure was determined by X-ray diffraction methods. Again, the ORTEP drawing of **7bM** reveals the presence of a ferrocenyl secondary phosphine oxide (Figure 3). The P═O bond is evidenced by its short bond length, 1.484(2) Å. A large coupling constant (J_{P-H} = 454.5 Hz) substantiates the existence of a P−H bond in **7bM**.

2.3. Reactions of 7bM with Pd(COD)Cl_2 and Pd(OAc)$_2$. The reaction of Pd(COD)Cl_2 with 2 equiv of (η^5-C_5H_4-P(═O)(^{t}Bu)(H))$_2$Fe (**7bM**) led to the formation of a palladium

(8) Intramolecular hydrogen bonding of related cases: (a) Wolf, C.; Lerebours, R. *Org. Lett.* **2004**, *6*, 1147–1150. (b) Cobley, C. J.; van den Heuvel, M.; Abbadi, A.; de Vries, J. G. *Tetrahedron Lett.* **2000**, *41*, 2467–2470. (c) Ref [6a].

dimer, [(**7b′M**)(**7b′M-H**$^+$)Pd(μ-Cl)]$_2$ (**8**), accompanied with the release of 2 molar equiv of HCl (Scheme 4). Note that the ligand used here, **7bM**, is a mixture of racemic forms. Compound **8** was characterized by spectroscopic methods as well as single-crystal X-ray diffraction. In ^{1}H NMR, singlets at 1.10 and 4.76 ppm were shown for the ^{t}Bu group and cyclopentadienyl ring, respectively. A set of multiplets around 4.40−4.65 ppm was assigned for the substituted cyclopentadienyl ring. The ^{31}P NMR spectrum also exhibited a singlet at 108.1 ppm. The crystal structure of **8** reveals that each palladium center is coordinated by two phosphinous acid ligands, though one of the ligand is deprotonated (Figure 4). There is an encapsulated diethyl ether molecule in each of the asymmetric units. A hydrogen bond between the oxygen atom (P═O) of the deprotonated phosphinous acid and the hydrogen atom (P−OH) of the phosphinous acid is observed.[8,6a] Two palladium metals are bridged by two chlorides. The four atoms Pd(1), Cl(1), Pd(2), Cl(2) are almost coplanar and in a diamond-shaped geometry. Two ferrocenyl moieties are above the plane; the other two are below the plane. The oxidation state of the palladium metal remains +2. The formation of **8** demonstrates that tautomerism indeed exists between ferrocenyl secondary phosphine oxide **7bM** and its phosphinous acid form **7b′M**. The latter form is responsible for the coordination toward the palladium metal.

Another reaction of 1 molar equiv of **7bM** with Pd(OAc)$_2$ was carried out in THF. The new product was characterized by spectroscopic methods as well as single-crystal X-ray diffraction. Unexpectedly, the crystal structure of [(**7b′M**)(**7b′M-H**$^+$)Pd(OAc)] (**9**) reveals that it is a bis-**7bM**-coordinated palladium acetate. It is believed that an original ligand/palladium = 1:1 complex was converted to the more stable complex **9** during the crystallization process. The palladium metal is in fact coordinated by two phosphinous acid ligands (Figure 5). The formation of the product was accompanied with the release of 1 molar equiv of HOAc. One was a ferrocenyl secondary phosphine oxide; the other a deprotonated ferrocenyl secondary phosphine oxide coordinated with palladium. One out of two acetates remained to chelate to palladium metal via η^2-means. The bond angle of O(3)−Pd−O(4) is 59.67(12)°. Two Pd−O bond lengths,

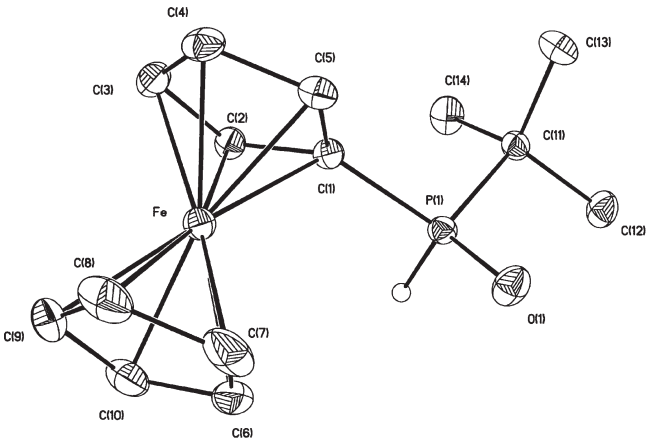

Figure 3. ORTEP drawing of **7bM**. Hydrogen atoms are omitted for clarity.

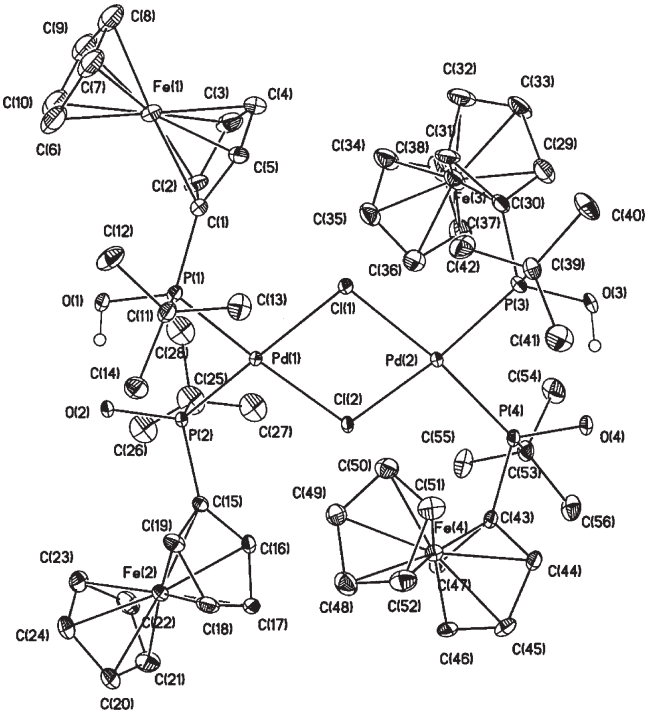

Figure 4. ORTEP drawing of **8**. Hydrogen atoms are omitted for clarity. Selected bond lengths (Å) and angles (deg): Pd(1)−P(1) 2.248(3); Pd(1)−P(2) 2.252(2); P(1)−O(1) 1.557(7); P(1)−Pd(1)−P(2) 92.57(9); Cl(1)−Pd(1)−Cl(2) 82.66(9); Pd(2)−Cl(1)−Pd(1) 97.23(9); O(1)−P(1)−C(1) 106.1(5); O(1)−P(1)−C(11) 106.0(5); C(1)−P(1)−C(11) 112.8(6); P(1)−O(1)−H(1A) 109.5.

Scheme 4. Preparations of Palladium Complexes from the Reactions 7bM with Pd(COD)Cl$_2$ and Pd(OAc)$_2$[a]

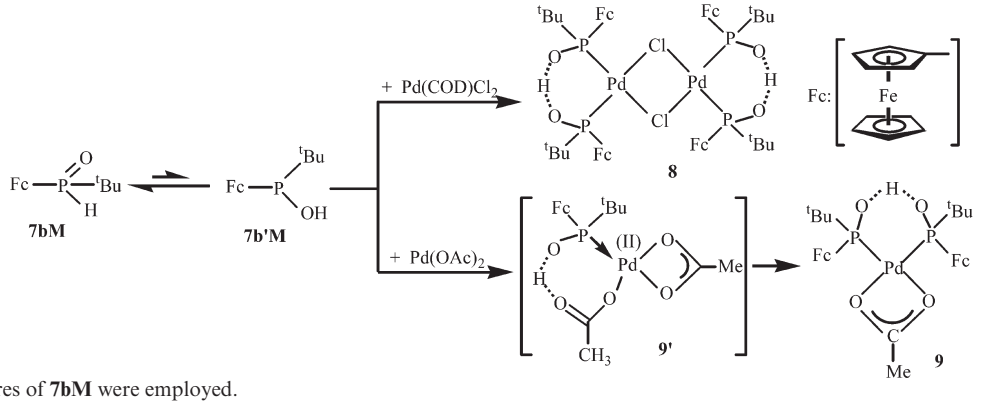

[a] Racemic mixtures of **7bM** were employed.

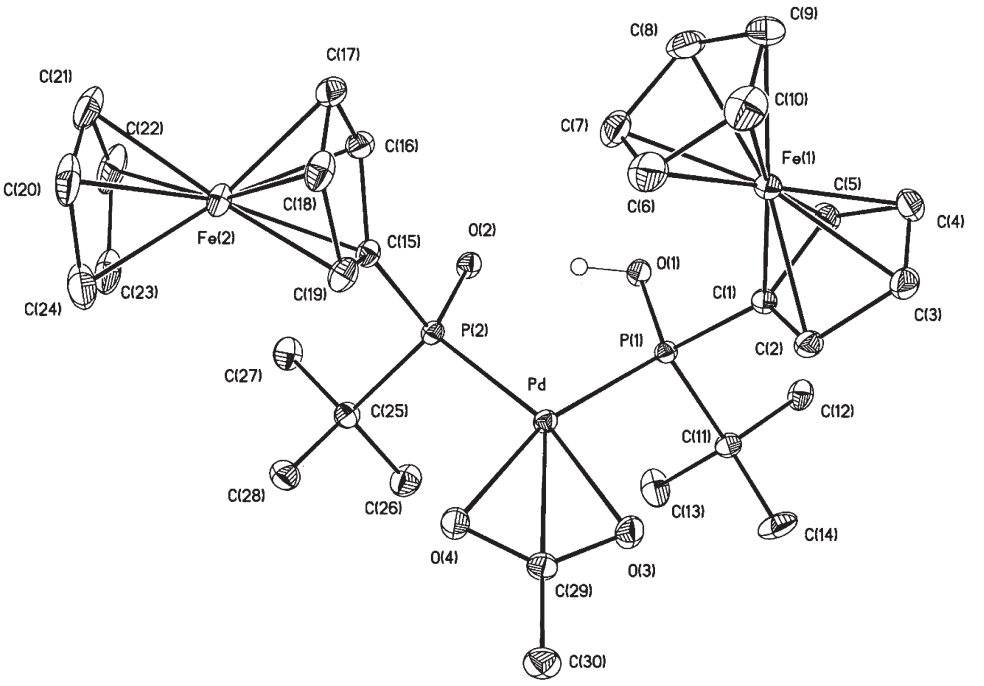

Figure 5. ORTEP drawing of **9**. Hydrogen atoms are omitted for clarity. Selected bond lengths (Å) and angles (deg): Pd−P(1) 2.2265(11); Pd−P(2) 2.2450(11); P(1)−O(1) 1.546(3); P(1)−Pd−P(2) 91.51(4); P(1)−O(1)−H(1A) 109.5; C(30)−C(29)−Pd 178.5(3); O(3)−Pd−O(4) 59.67(12).

2.181(3) and 2.194(3) Å, from acetate to palladium are almost the same. Again, intramolecular hydrogen bondings between deprotonated and non-deprotonated ferrocenyl secondary phosphine oxides were observed.[8,6a] The bond length of P═O is 1.546(3) Å, indicating the existence of a double bond. The two bonds between P and Pd can be regarded as one dative bond plus a covalent bond. The six atoms Pd, P(1), P(2), O(3), O(4), and C(29) are almost coplanar. Two ferrocenyl moieties are on the same side of the plane; two ^{t}Bu groups are on the other side. The bond angle of P(1)−Pd−P(2) is 91.51(4)°. The charge of the palladium metal remains +2. Judging from the ^{1}H and ^{31}P NMR spectra of **9**, the two ligands are in slightly different environment. Although secondary phosphine oxide chelated $PdCl_2$ complexes are known,[8a] to the best of our knowledge this is the first example of a two secondary phosphine oxide ligand coordinated Pd(II)(OAc) complex.[9]

2.4. Application of 7aB in Palladium-Catalyzed Suzuki−Miyaura Reactions. As demonstrated, the best performance of a palladium-catalyzed carbon−carbon cross-coupling reaction can be achieved by optimizing the major factors involved.[10] Palladium-catalyzed Suzuki−Miyaura reactions of bromobenzene with 4-bromobenzaldehyde were carried out by employing **7aB** as ligand precursor (Scheme 5).

To begin with, the efficiencies of several commonly used palladium sources were screened. Suzuki−Miyaura reactions of 4-bromotoluene and phenylboronic acid employing **7aB** with various Pd sources in a K_2CO_3/THF system were carried out at 60 °C for 15 h (Table 1). As shown, the best yield was obtained while using $Pd(OAc)_2$ as the palladium source (entry 1). This is a consistently common observation.[11]

Scheme 5. Secondary Phosphine Oxide Assisted Palladium-Catalyzed Suzuki−Miyaura Reactions

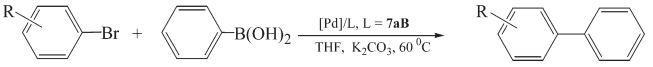

Table 1. Suzuki−Miyaura Coupling Reactions Employed Various Palladium Sources[a]

entry	palladium source	NMR conv (%)[b]
1	$Pd(OAc)_2$	94
2	$Pd_2(dba)_3$	83
3	$PdCl_2$	88
4	$PdCl_2(CH_3CN)_2$	71
5	$[(\eta^3\text{-}C_3H_5)PdCl]_2$	46
6	$Pd(COD)Cl_2$	40

[a] Conditions: 1.0 mmol of 4-bromobenzaldehyde, 1.5 mmol of phenylboronic acid, 2.0 mmol of K_2CO_3, 1 mL of THF, and 1 mol % Pd/**7aB**, Pd/**7aB** = 1:1, 60 °C, 15 h. [b] Determined by ^{1}H NMR.

The ratio of ligand to metal is also a critical factor in the ligand-assisted palladium complex-catalyzed cross-coupling reactions. Conventionally, the ratio of **7aB**/$Pd(OAc)_2$ should be 1:1 according to the presumed composition of the active catalyst precursor. The impact of the **7aB**/$Pd(OAc)_2$ ratio on the catalytic efficiency was evaluated here. In order to be able to differentiate the performances of the catalytic reactions, a less efficient 4-bromotoluene rather than 4-bromobenzaldehyde was employed. Unexpectedly, better catalytic efficiencies are shown for the ratio of **7aB**/$Pd(OAc)_2$ greater than 1.

(9) Amoroso, D.; Bell, A.; Protasiewicz, J. D. *Organometallics* **2005**, *24*, 4099–4102.

(10) (a) Goldman, E. R.; Medintz, I. L.; Whitley, J. L.; Hayhurst, A.; Clapp, A. R.; Uyeda, H. T.; Deschamps, J. R.; Lassman, M. E.; Mattoussi, H. *J. Am. Chem. Soc.* **2005**, *127*, 6744–6751. (b) Braga, A. A. C.; Morgon, N. H.; Ujaque, G.; Maseras, F. *J. Am. Chem. Soc.* **2005**, *127*, 9298–9307.

(11) (a) Amatore, C.; Jutand, A. *Acc. Chem. Res.* **2000**, *33*, 314–321. (b) Amatore, C.; Carré, E.; Jutand, A.; M'Barki, M. A.; Meyer, G. *Organometallics* **1995**, *14*, 5605–5614.

Table 2. Suzuki−Miyaura Coupling Reactions Employing Various $Pd(OAc)_2$/7aB[a]

entry	[Pd]/**7aB**	NMR conv (%)[b]
1	1/0	11
2	1/0.5	49
3	1/1	55
4	1/2	62
5	1/3	68
6	1/1	58[c]
7	1/2	64[c]
8	1/3	73[c]

[a] Conditions: 1.0 mmol of 4-bromotoluene, 1.5 mmol of phenylboronic acid, 2.0 mmol of K_2CO_3, 1 mL of THF, and 1 mol % $Pd(OAc)_2$, 19 h, 60 °C. [b] Determined by ^{1}H NMR, average of two runs. [c] 24 h.

Table 3. Suzuki−Miyaura Coupling Reactions Employing Various Bases[a]

entry	base	time (h)	NMR conv (%)[b]
1	NaO^tBu	4	90
2	NaO^tBu	12	>99
3	K_3PO_4	19	88
4	KOH	19	88
5	CsF	19	80
6	KO^tBu	19	78
7	NaOH	19	66
8	K_2CO_3	19	52
9	KF	19	29
10	Cs_2CO_3	19	27
11	CsOH	19	14

[a] Conditions: 1.0 mmol of 4-bromotoluene, 1.5 mmol of phenylboronic acid, 2.0 mmol of base, 1 mL of THF, and 1 mol % $Pd(OAc)_2$, Pd:**7aB** = 1:1, 50 °C. [b] Determined by ^{1}H NMR.

The optimum ratio might even be as high as 3:1 (Table 2, entries 1−5). In order to increase the amount of **7a′B**, the effective phosphine form in the coordination toward palladium center, a large excess of **7aB** is needed. This can be explained by the imbalanced tautomeric equilibrium that favors **7aB** over **7a′B**. Otherwise, long reaction hours did not improve the yield (entries 6−9).

As demonstrated, the type of base employed in the Suzuki−Miyaura reaction is crucial to the catalytic efficiency.[12] It is also the most unpredictable element among all the factors that affect performance. The influence of the bases used in these secondary phosphine oxide-catalyzed coupling reactions was examined (Table 3). As shown, the best result came with NaO^tBu used as the active base.

The solubility of substances and catalyst in solvent is greatly affected by the polarity. A careful selection of appropriate solvent is critical to the performance of the catalytic reaction. Interestingly, the best result was observed in aqueous solution using Na^tOBu as base (Table 4, entry 2). This might be partly attributed to the formation of highly polar deprotonated **7a′B**-chelated palladium complex in base media, which is best dissolved in water. Since the organic reactants are not particularly soluble in aqueous solution, the ^{t}BuOH, yielded from the addition of Na^tOBu in water, is responsible for their dissolubility in solution. A careful examination by varying the ratio of ^{t}BuOH/H_2O in either NaO^tBu or NaOH as base (entries 9−14) found that the yields are rather poor without the presence of ^{t}BuOH

Table 4. Suzuki−Miyaura Coupling Reactions Employing Various Solvent Ratios and Bases[a]

entry	solvent	base	time (h)	NMR conv (%)[b]
1	H_2O	NaO^tBu	2	91
2	H_2O	NaO^tBu	4	>99
3	THF	NaO^tBu	4	91
4	CH_3OH	NaO^tBu	4	89
5	1,4-dioxane	NaO^tBu	4	78
6	toluene	NaO^tBu	4	35
7	DMF	NaO^tBu	4	11
8	CH_3CN	NaO^tBu	4	1
9	^{t}BuOH/H_2O (0:1)	NaO^tBu	2	70
10	^{t}BuOH/H_2O (0:1)	NaOH	2	0
11	^{t}BuOH/H_2O (1:0)	NaO^tBu	2	14
12	^{t}BuOH/H_2O (1:0)	NaOH	2	21
13	^{t}BuOH/H_2O (0.5:0.5)	NaO^tBu	2	53
14	^{t}BuOH/H_2O (0.5:0.5)	NaOH	2	69
15	H_2O (1 mL)	NaO^tBu	1	52 (70)[c]
16	H_2O (2 mL)	NaO^tBu	1	39 (56)[c]
17	H_2O (3 mL)	NaO^tBu	1	26 (52)[c]

[a] Conditions for entries 1−8: 1.0 mmol of 4-bromotoluene, 1.5 mmol of phenylboronic acid, 2.0 mmol of base, 1 mL of solvent, and 1 mol % $Pd(OAc)_2$/**7aB** = 1:1, 50 °C; 40 °C for entries 9−14. [b] Determined by ^{1}H NMR. [c] 2 h.

either by adding it directly or produced indirectly from the reaction with water. In addition, the concentration of the reactant, by changing the amount of solvent, indeed affects the rate of the reaction (entries 15−17). A more concentrated solution leads to the better performance.

It was also a common observation that in Suzuki−Miyaura coupling reactions a better conversion is achieved with aryl halides bearing an electron-withdrawing than with an electron-donating substituent.[13] In fact, this is mostly correct for the reaction with the oxidative addition process as the rate-determining step (rds).[14] As shown in Table 5, less effective performances were observed for substances with electron-donating groups than the unsubstituted case (entries 2−5 vs 1). Nevertheless, the steric effect plays a more critical role than the electronic effect here (entries 6, 7). Unfortunately, this system does not work well for the cases of aryl chlorides (entries 8−10).

2.5. Application of 7bM in Palladium-Catalyzed Suzuki−Miyaura Reactions. In principle, **7bM** should act as a monodentate ligand. Its reactivity is expected to be different from that of the disubstituted **7aB**. Suzuki−Miyaura reactions were carried out with **7bM** employed as ligand. Several factors that might be crucial to the performance were examined. First, the efficiencies of several commonly used palladium sources were screened. Here, Suzuki−Miyaura reactions of 4-bromoaldehyde and phenylboronic acid employing **7bM** with various Pd sources in a K_2CO_3/THF system were carried out at 60 °C for 7 h (Table 6). In order to differentiate the reactivities of various palladium sources, a less efficient base, K_2CO_3, was used. As shown, the best yield was obtained when using $Pd(OAc)_2$ as the palladium source (entry 1).

Since various bonding modes are possible for different types of ligands, the ratio of ligand to palladium is also crucial in Suzuki−Miyaura coupling reactions. Suzuki−Miyaura

(12) (a) Dubbaka, S. R.; Vogel, P. *Org. Lett.* **2004**, *6*, 95–98. (b) Grasa, G. A.; Hillier, A. C.; Nolan, S. P. *Org. Lett.* **2001**, *3*, 1077–1080. (c) Miyaura, N.; Yamada, K.; Suginome, H.; Suzuki, A. *J. Am. Chem. Soc.* **1985**, *107*, 972–980.

(13) Kataoka, N.; Shelby, Q.; Stambuli, J. P.; Hartwig, J. F. *J. Org. Chem.* **2002**, *67*, 5553–5566.

(14) (a) Singh, R.; Viciu, M. S.; Kramareva, N.; Navarro, O.; Nolan, S. P. *Org. Lett.* **2005**, *7*, 1829–1832. (b) Limmert, M. E.; Roy, A. H.; Hartwig, J. F. *J. Org. Chem.* **2005**, *70*, 9364–9370. (c) Xiong, Z.; Wang, N.; Dai, M.; Li, A.; Chen, J.; Yang, Z. *Org. Lett.* **2004**, *6*, 95–98. (d) Dai, C.; Fu, G. C. *J. Am. Chem. Soc.* **2001**, *123*, 2719–2724.

Table 5. Suzuki−Miyaura Coupling Reactions Employing Various Aryl Halides[a]

Entry	Substrate	Product	Yield (%)[b]
1		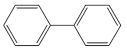	95
2	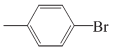	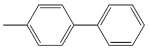	93
3		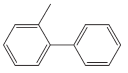	94
4	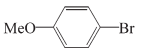	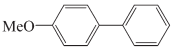	79
5	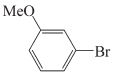	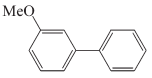	74
6		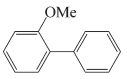	49
7	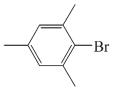	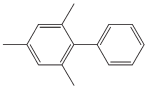	47
8	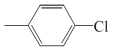	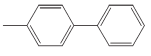	NR
9	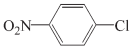	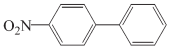	18[c]
10	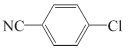	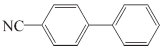	5[c]

[a] Conditions: 1.0 mmol of aryl bromide, 1.5 of mmol phenylboronic acid, NaO^tBu 2.0 mmol, H_2O 1 mL, and 1 mol % $Pd(OAc)_2$, Pd:L = 1:1, 60 °C, 2 h. [b] Isolated yield, average of two runs. [c] NMR conversion.

Table 6. Suzuki−Miyaura Coupling Reactions Employed Various Palladium Sources[a]

entry	palladium source	NMR conv (%)[b]
1	$Pd(OAc)_2$	77
2	$Pd_2(dba)_3$	54
3	$PdCl_2$	57
4	$PdCl_2(CH_3CN)_2$	69
5	$[(\eta^3\text{-}C_3H_5)PdCl]_2$	10
6	$Pd(COD)Cl_2$	38

[a] Conditions: 1.0 mmol of 4-bromobenzaldehyde, 1.5 mmol of phenylboronic acid, 2.0 mmol of K_2CO_3, 1 mL of THF, and 1 mol % palladium salt, [Pd]/**7bM** = 1:1, 60 °C, 7 h. [b] Determined by ^1H NMR.

coupling reactions were carried out *in situ* by employing various ratios of **7bM**/$Pd(OAc)_2$. A less efficient 4-bromotoluene was used than 4-bromobenzaldehyde to discriminate the performances of various ratios of ligand to palladium salt system (Table 7). Unexpectedly, the best yield was obtained with **7bM**/$Pd(OAc)_2$ = 1:1 (entries 2 and 6). The catalytic performances are consistently better for systems fixed in this ratio even with different reaction times.

Subsequently, the impact of the base used in the reaction was examined (Table 8). Among all the bases used, NaO^tBu and K_3PO_4 were found to be more effective when

Table 7. Suzuki−Miyaura Coupling Reactions Employing Various $Pd(OAc)_2$/7bM [a]

entry	[Pd]/**7bM**	NMR conv (%)[b]
1	1:0	9
2	1:1	36
3	1:2	27
4	1:3	29
5	1:0	15[c]
6	1:1	84[c]
7	1:2	57[c]
8	1:3	68[c]

[a] Conditions: 1.0 mmol of 4-bromotoluene, 1.5 mmol of phenylboronic acid, 2.0 mmol of K_2CO_3, 1 mL of THF, and 1 mol % $Pd(OAc)_2$, 4 h, 60 °C. [b] Determined by ^1H NMR, average of two runs. [c] 24 h.

Table 8. Suzuki−Miyaura Coupling Reactions Employing Various Bases[a]

entry	base	time (h)	NMR conv (%)[b]
1	NaO^tBu	1	67
2	K_2CO_3	1	7
3	NaOH	1	19
4	K_3PO_4	1	72
5	NaO^tBu	2	>99
6	K_2CO_3	2	10
7	NaOH	2	28
8	K_3PO_4	2	90
9	NaO^tBu	2	68
10	K_3PO_4	2	19
11	NaO^tBu	4	70
12	K_3PO_4	4	27

[a] Conditions: 1.0 mmol of 4-bromotoluene (entries 1−8) or 4-bromoanisole (entries 9−12), 1.5 mmol of phenylboronic acid, 2.0 mmol of base, 1 mL of THF, and 1 mol % $Pd(OAc)_2$, [Pd]:**7bM** = 1:1, 60 °C. [b] Determined by ^1H NMR.

Table 9. Suzuki−Miyaura Coupling Reactions Employing Various Solvent[a]

entry	solvent	time (h)	NMR conv (%)[b]
1	THF	1	67
2	toluene	1	61
3	H_2O	1	NR
4	CH_3OH	1	77
5	1,4-dioxane	1	40
6	DMF	1	22
7	THF	2	94
8	toluene	2	63
9	H_2O	2	NR
10	CH_3OH	2	80
11	1,4-dioxane	2	62
12	DMF	2	34

[a] Conditions: 1.0 mmol of 4-bromotoluene, 1.5 mmol of phenylboronic acid, 2.0 mmol of base, 1 mL of solvent, 1 mol % $Pd(OAc)_2$, [Pd]:**7bM** = 1:1, 60 °C. [b] Determined by ^1H NMR.

the reaction was run in THF with 4-bromotoluene (entries 1−8). Again, a less efficient 4-bromoanisole, rather than 4-bromotoluene, was used to differentiate the reactivities of these two bases (entries 9−12). It was found that NaO^tBu is more effective than K_3PO_4 in this case.

The effects of solvents used in the coupling reaction were evaluated also (Table 9). The best yield was observed using THF as the solvent (entry 7). Although their polarities are close, 9.8 for 1,4-dioxane and 9.1 for THF, the catalytic performances are quite different. Water is not an adequate solvent due to poor solubility and hydrolysis of the ligand (entries 3 and 9).

The following table shows the results from the **7bM**-assisted Suzuki−Miyaura cross-coupling reactions with

Table 10. Suzuki−Miyaura Coupling Reactions Employing Various Aryl Halides[a]

Entry	Substrate	Product	Yield (%)[b]
1		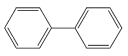	>99
2	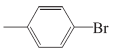	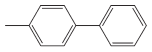	87
3		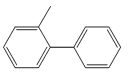	90
4	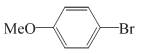	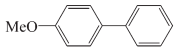	86
5	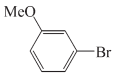	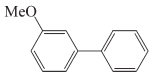	69
6		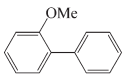	56
7	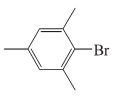	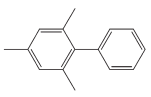	47
8		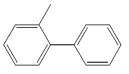	9[c]
9	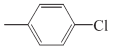	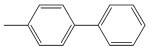	16[c]
10	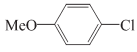	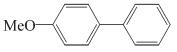	5[c]
11	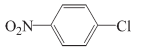	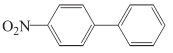	38[c]
12	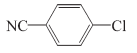	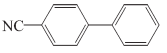	33[c]

[a] Conditions: 1.0 mmol of aryl bromide, 1.5 mmol of phenylboronic acid, NaO^tBu 2.0 mmol, THF 1 mL, and 1 mol % $Pd(OAc)_2$, [Pd]:**7bM** = 1:1, 60 °C, 1 h. [b] Isolated yield; average of two runs. [c] NMR conversion.

substituted aryl bromides (Table 10). It was less effective for the substrate with an electron-donating group. As expected, the catalytic efficiency was lower when the substrate bearing substituent had severe steric hindrance (entry 7). Nevertheless, an unexpected good performance was observed for 2-bromotoluene (entry 3). Less effective performances for the cases of aryl chlorides were observed (entries 8−12). Good to excellent yields were reported by Wolf for the POPd- or POPd1-catalyzed Suzuki−Miyaura cross-coupling of 4-chloroquinoline derivatives and boronic acid. Here, POPd and POPd1 stand for *trans*-$[(^tBu)_2P(OH)]_2$-$PdCl_2$ and $[[(^tBu)_2P(OH)(^tBu)_2PO)]PdCl]_2$, respectively. The reactions were carried out in 1,4-dioxane at 100 °C for 20 h.[6g] Recent work of Li showed similar efficiency in Suzuki−Miyaura cross-coupling of aryl halides and 6-methoxypyridyl-2-boronic ester using PXPd, *trans*-$[(^tBu)_2PCl]_2$-$PdCl_2$, as the catalyst precursor.[5a]

The crystal structures of both **8** and **9** reveal that the ratio of the coordinated ligand to the palladium metal is 2:1. Nevertheless, the before-mentioned work shows that the catalytic performance is better with an equal ratio of ligand and palladium. However, the composition of a crystallized compound may not necessarily represent the true formula of the catalytically active species. In an ^{31}P NMR experiment, the **7bM**-coordinated catalytically active species was monitored while adding **7bM** to $Pd(OAc)_2$ in the ratio of 1:1. Initially, a signal was observed in the ^{31}P NMR at 118 ppm; this slowly changed to 108 ppm in 60 °C within 1 h. Precipitation of gray metal particles, presumably aggregated palladium black, was observed along with the change of the NMR signal. Latterly, the composition of the palladium complex in solution was identified as **9** by ^{31}P NMR measurement since it showed identical chemical shift to that of **9** from a purified crystalline form. The unstable catalytic precursor **9′**, which is responsible for the chemical shift at 118 ppm, was proposed as the original product (Scheme 4). Presumably, it converted to **9** by the process of disproportionation and elimination of part of the palladium moiety. It is assumed that all these potentially catalytic precursors have the divalent palladium metal in the center of a tetracoordinated, square-planar environment. These Pd(II) species are all be reduced to Pd(0) before the catalytic cycle starts.

Summary. We have developed a general route for the preparation of ferrocenyl secondary phosphine oxides. They have been employed as phosphine ligands through tautomeric equilibrium in basic media and proven themselves to be fairly efficient in the palladium-catalyzed Suzuki−Miyaura reaction. Since the secondary phosphine oxides are not prone to oxidation, employment of secondary phosphine oxides is an applicable choice for the purpose of long-term storage.

3. Experimental Section

3.1. General. All operations were performed in a nitrogen-flushed glovebox or in a vacuum system. Freshly distilled solvents were used. All processes of separations of the products were performed by centrifugal thin layer chromatography (CTLC, Chromatotron, Harrison model 8924) or column chromatography. GC analyses were performed on a HP-5890 FID GC with a QUADREX 007-CW fused silica 30 m column, and data were recorded on a HP ChemStation. Most of the ^1H NMR spectra were recorded on a 300 MHz Varian VXR-300S spectrometer. The chemical shifts are reported in ppm relative to internal standards $CHCl_3$ (δ = 7.26), CH_2Cl_2 (δ = 5.30), or $CH_3C(=O)CH_3$ (δ = 2.09). ^{31}P and ^{13}C NMR spectra were recorded at 121.44 and 75.46 MHz, respectively. The chemical shifts for the former and the latter are reported in ppm relative to internal standards H_3PO_4 (δ = 0.0) and $CHCl_3$ (δ = 77) or CH_2Cl_2 (δ = 53), respectively. In addition, some routine ^1H NMR spectra were recorded on either a Gemini-200 spectrometer at 200.00 MHz or a Varian-400 spectrometer at 400.00 MHz. Mass spectra were recorded on a JEOL JMS-SX/SX 102A GC/MS/MS spectrometer. Elemental analyses were recorded on a Heraeus CHN-O-S-Rapid.

3.2. Synthesis and Characterization of 7aB. A 100 mL round-bottomed flask charged with a magnetic stir bar was placed with 2.00 mmol of ferrocene (0.372 g) and 12 mL of hexanes. The solution was kept stirring at 0 °C while 2.2 molar equiv of n-BuLi and TMEDA were slowly added. After 0.5 h the solution was allowed to warm to 25 °C and stirred for another 8 h. A dark red solid, 1,1′-dilithioferrocene, was obtained after the removal of solvent under reduced pressure.

In a drybox, dichlorophenylphosphine (2.00 mmol, 0.358 g) and bis(diethylamino)phenylphosphine (2.00 mmol, 0.505 g)

were dissolved in 2.5 mL of THF separately in 50 mL flasks. Then, these two solutions were mixed and stirred at 25 °C for 1.5 h. A colorless oily product, chloro(diethylamino)phenylphosphine, resulted.

At 0 °C, chloro(diethylamino)phenylphosphine was added to the solution of 1,1′-dilithioferrocene, in 10 mL of THF. The solution was allowed to warm to 25 °C and stirred for another 5 h. Subsequently, the solvent was removed under reduced pressure and the residue was separated by CTLC. A dark yellow colored band was eluted using a mixed solvent mobile phase ($MeOH/CH_2Cl_2$ = 1:6) and was identified as (η^5-C_5H_4-P(=O)-(Ph)(H))$_2$Fe, **7aB**. The yield of **7aB** is 68.4% (0.594 g, 1.37 mmol).

Selected Spectroscopic Data for 7aB. ^{1}H NMR ($CDCl_3$, δ/ppm): 4.49−4.83 (m, 8 H, (η^5-C_5H_4)$_2$), 7.47−7.73 (m, 10 H, Ph), 7.92, 8.02 (d, 2 H, P−H, J_{P-H} = 487.3, 489.3 Hz). ^{13}C NMR ($CDCl_3$, δ/ppm): 72.5−73.3 (m, 10 C, (η^5-C_5H_4)$_2$), 128.6−132.1 (m, 12 C, Ph). ^{31}P NMR ($CDCl_3$, δ/ppm): 19.2 (d, 2 P, P−H, J_{P-H} = 489.4 Hz). MS (FAB): m/z = 432 (M^+). Anal. Calcd: C, 60.86; H, 4.64. Found: C, 59.50; H, 4.44.

3.3. Synthesis and Characterization of 7aM, 7bM, and 7cM. A 100 mL round-bottomed flask charged with a magnetic stir bar was placed with 4.00 mmol of ferrocene (0.372 g) and 10 mL of THF. The solution was kept stirring at 0 °C while 4.4 equiv of 1.9 mL of *t*-BuLi (2.3 M in penteane, 4.4 mmol) was slowly added. After 1.0 h the solution was allowed to warm to 25 °C and stirred for another 3 h. A dark red solid, 1,1′-dilithioferrocene, was obtained after the removal of solvent under reduced pressure.

First, 2.00 mol of *tert*-butyldichlorophosphine was dissolved in 2.5 mL of THF. Then it was added to the solution of 1,1′-dilithioferrocene at 25 °C. The solution was allowed to warm to room temperature and stirred for another 12 h at 60 °C. Subsequently, the solution was allowed to cool to room temperature, and a small amount of water was added to quench the reaction. The organic portion was collected from the separatory funnel after washing with ethyl acetate several times. Then, the solvent was removed under reduced pressure, and the residue was separated by CTLC. A dark yellow colored band was eluted using a mixed solvent mobile phase (EA/CH_2Cl_2 = 3:1) and was identified as (η^5-C_5H_4-P(=O)(Ph)(H))$_2$Fe, **7bM**. The same procedures were executed for the preparations of **7aM** and **7cM** except the starting materials were dichlorophenylphosphine and dichlorocyclohexylphosphine, respectively. The yields of **7aM**, **7bM**, and **7cM** were 34% (0.210 g, 0.68 mmol), 64% (0.185 g, 1.28 mmol), and 46% (0.290 g, 0.92 mmol), respectively.

Selected Spectroscopic Data for 7aM. ^{1}H NMR ($CDCl_3$, δ/ppm): 4.33 (s, 5 H, η^5-C_5H_5), 4.44−4.48 (m, 4 H, η^5-C_5H_4), 7.48−7.76 (m, 5 H, Ph), 8.03 (d, 1 H, P−H, J_{P-H} = 483.3 Hz). ^{13}C NMR ($CDCl_3$, δ/ppm): 69.6 (s, 5 C, Cp), 70.4−71.9 (m, 5 C, Cp), 128.5−132.1 (m, 6 C, Ph). ^{31}P NMR ($CDCl_3$, δ/ppm): 19.8 (d, 1 P, P−H, J_{P-H} = 484.5 Hz). MS (FAB): m/z = 310 (M^+). Anal. Calcd: C, 61.97; H, 4.88. Found: C, 60.33; H, 5.63.

Selected Spectroscopic Data for 7bM. ^{1}H NMR ($CDCl_3$, δ/ppm): 1.10 (d, J_{P-H} = 16.8 Hz, 9 H), 4.36 (s, 5 H), 4.27−4.62 (m, 4 H), 6.88 (d, J_{P-H} = 454.5 Hz, 1 H). ^{13}C NMR ($CDCl_3$, δ/ppm): 23.2, 32.6 (d, J_{P-C} = 71.1 Hz), 67.6(d, J_{P-C} = 110.1 Hz), 70.31, 71.2 (d, J_{P-C} = 37.5 Hz), 72.2 (d, J_{P-C} = 33.1 Hz). ^{31}P NMR ($CDCl_3$, δ/ppm): 47.5(s). (d, 1 P, P−H, J_{P-H} = 454.0 Hz). MS (FAB): m/z = 290 (M^+). Anal. Calcd.: C, 57.96; H, 6.60. Found: C, 56.84; H, 6.65.

Selected Spectroscopic Data for 7cM. ^{1}H NMR ($CDCl_3$, δ/ppm): 1.21 (d, 4 H), 1.67 (m, 6 H), 4.36 (s, 5 H), 4.13−4.62 (m, 4 H), 7.06 (d, J_{P-H} = 458.5 Hz, 1 H). ^{13}C NMR ($CDCl_3$, δ/ppm): 25.0 (d, J_{P-C} = 9.1 Hz), 25.9 (d, J_{P-C} = 15.2 Hz), 39.4 (d, J_{P-C} = 72.6 Hz), 68.3 (d, J_{P-C} = 103.8 Hz), 69.6, 71.3 (d, J_{P-C} = 10.9 Hz), 71.6 (d, J_{P-C} = 9.1 Hz). ^{31}P NMR ($CDCl_3$, δ/ppm): 37.3(d, 1 P, P−H, J_{P-H} = 457.8 Hz). MS (FAB): m/z = 316 (M^+). Anal. Calcd: C, 60.78; H, 6.70. Found: C, 59.72; H, 6.86.

3.4. Synthesis and Characterization of 8. In a N_2-flashed 100 mL round-bottomed flask, 0.290 g (0.100 mmol) of **7bM** and 0.285 g (0.10 mmol) of $Pd(COD)Cl_2$ were placed with 8 mL of CH_2Cl_2. The solution was kept stirring at 60 °C for 1 h before the solvent was removed under reduced pressure, and the residue was separated by CTLC. A red-colored band was eluted using a mixed solvent mobile phase (EA/CH_2Cl_2 = 10:1) and was identified as [(**7b′M**)(**7b′M-H**$^+$)Pd(μ-Cl)]$_2$, **8**. The yield of **8** is 86% (0.064 g, 0.043 mmol).

Selected Spectroscopic Data for 8. ^{1}H NMR ($CDCl_3$, δ/ppm): 1.10 (d, J_{P-H} = 14.8 Hz, 36 H), 4.76 (s, 20 H), 4.40−4.65 (m, 16 H). ^{13}C NMR ($CDCl_3$, δ/ppm): 72.8 (s, 20 C, Cp), 70.6, 70.1, 69.1 (t, 20 C, Cp), 41.2, 41.0, 40.7 (t, 12 C, −$C(CH_3)_3$), 27.1 (s, 4 C, −$C(CH_3)_3$). ^{31}P NMR ($CDCl_3$, δ/ppm): 108.1. MS (FAB): m/z = 1442 ($M - {}^tBu - OH)^+$. Anal. Calcd: C, 46.64; H, 5.17. Found: C, 45.86; H, 5.24.

3.5. Synthesis and Characterization of 9. In a N_2-flashed 100 mL round-bottomed flask, 0.290 g (0.10 mmol) of **7bM** and 0.224 g (0.10 mmol) of $Pd(OAc)_2$ were placed with 8 mL of THF. The solution was kept stirring at 60 °C for 1 h before the solvent was removed under reduced pressure, and the residue was separated by CTLC. A red-colored band was eluted using a mixed solvent mobile phase (EA/CH_2Cl_2 = 20:1) and was identified as [(**7b′M**)(**7b′M-H**$^+$)Pd(OAc)], **9**.

Selected Spectroscopic Data for 9. ^{1}H NMR ($CDCl_3$, δ/ppm): 1.28 (d, J_{P-H} = 16.8 Hz, 9 H), 1.18 (d, J_{P-H} = 17.2 Hz, 9 H), 2.05 (s, 3 H), 4.16−4.58 (m, 18 H). ^{13}C NMR ($CDCl_3$, δ/ppm): 72.4 (s, 10 C, Cp), 70.6, 69.9, 67.8 (t, 10 C, Cp), 39.9, 39.3, 38.7 (t, 6 C, −$C(CH_3)_3$), 26.9−24.1 (m, 2 C, −$C(CH_3)_3$). ^{31}P NMR (toluene-d_6, δ/ppm): 104.0, 105.5. MS (FAB): m/z = 685 ($M - CH_3COO)^+$.

3.6. General Procedures for the Suzuki−Miyaura Cross-Coupling Reactions. Suzuki−Miyaura cross-coupling reactions were performed according to the following procedures. Reactants including **7aB** (8.78 mg, 0.01 mmol), phenylboronic acid (0.183 g, 1.50 mmol), and NaOH (0.120 g, 3.00 mmol) were placed into a 20 mL Schlenk flask. The flask was evacuated and backfilled with nitrogen before adding toluene (1.0 mL) and 2-bromothiophene (0.11 mL, 1.00 mmol). The solution was stirred at 40 °C for 3 h. Subsequently, an excess amount of water was added and the product was extracted with ether (3 × 20 mL). The combined organic extracts were dried over anhydrous $MgSO_4$ and concentrated under vacuum. The crude residue was purified by flash chromatography on silica gel. Similar procedures are applied to the case of **7aM**.

3.7. X-ray Crystallographic Studies. Suitable crystals of **7aB**, **7aM**, **7bM**, **8**, and **9** were sealed in thin-walled glass capillaries under a nitrogen atmosphere and mounted on a Bruker AXS SMART 1000 diffractometer. Intensity data were collected in 1350 frames with increasing ω (width of 0.3° per frame). The absorption correction was based on the symmetry equivalent reflections using the SADABS program. The space group determination was based on a check of the Laue symmetry and systematic absences and was confirmed using the structure solution. The structure was solved by direct methods using the SHELXTL package.[15] All non-H atoms were located from successive Fourier maps, and hydrogen atoms were refined using a riding model. Anisotropic thermal parameters were used for all non-H atoms, and fixed isotropic parameters were used for H atoms.[16] Crystallographic data for compounds **7aB**, **7aM**, **7bM**, **8**, and **9** are available from the Supporting Information.

Acknowledgment. We thank the National Science Council of the ROC (grant NSC 95-2113-M-005-015-MY3) for financial support.

(15) Sheldrick, G. M. *SHELXTL PLUS User's Manual, Revision 4.1*; Nicolet XRD Corporation: Madison, WI, 1991.

(16) The hydrogen atoms were riding on carbons or oxygens in their idealized positions and held fixed with C−H distances of 0.96 Å.

Supporting Information Available: Crystallographic data for the structural analysis have been deposited with the Cambridge Crystallographic Data Center, CCDC nos. 678966, 678967, 719989, 719989, and 719991 for compound **7aB**, **7aM**, **7bM**, **8**, and **9**, respectively. Copies of this information may be obtained free of charge from the Director, CCDC, 12 Union Road, Cambridge CB2 1EZ, UK (fax: +44-1223-336033; e-mail: deposit@ccdc.cam.ac.uk or www: http://www.ccdc.cam.ac.uk). These files in CIF format for **7aB**, **7aM**, **7bM**, **8**, and **9** and spectroscopic data, ^{1}H, ^{13}C, ^{31}P NMR, MS, and EA for new compounds are available free of charge via the Internet at http://pubs.acs.org.